Journal of
*Marine Science and Engineering*

MDPI

# Acoustic Pressure, Particle Motion, and Induced Ground Motion Signals from a Commercial Seismic Survey Array and Potential Implications for Environmental Monitoring

**Robert D. McCauley [1], Mark G. Meekan [2] and Miles J.G. Parsons [2,*]**

[1] Centre for Marine Science and Technology, Curtin University, Bentley, Western Australia, 6109: r.mccauley@curtin.edu.au
[2] Australian Institute of Marine Science, Perth, Western Australia, 6009; m.meekan@aims.gov.au
* Correspondence: m.parsons@aims.gov.au; Tel.: +61 (8) 6369 4053

## Supplementary Material

*Propagation conditions at experimental sites*

In April 2018, five months prior to the exposure experiment, a survey was conducted to map the experimental area to better understand the local transmission characteristics. At this time, a R2Sonic 2026 multi-beam echosounder (MBES) sonar survey was conducted to map the bathymetry and characterize seafloor 'hardness' at the two experimental locations (Figure S1). Together with towed video and sediment grab validation data, the multi-beam backscatter confirmed that the seafloor was composed of a layer of sand over hard substrate, likely limestone, allowing growth of sessile benthic organisms (sponges, gorgonians, some corals, etc.) where the sand layer was thin. This layer was thinner at the northern site than the southern, often leading to exposed rocks around the shallow shoals (Figure S1b). In the MBES backscatter these 'hard' habitats displayed a higher return at 100 kHz, the lowest operational frequency. Where a thick layer of sand existed over the limestone bed, the acoustic reflection was weaker and only sand waves or ripples were present.

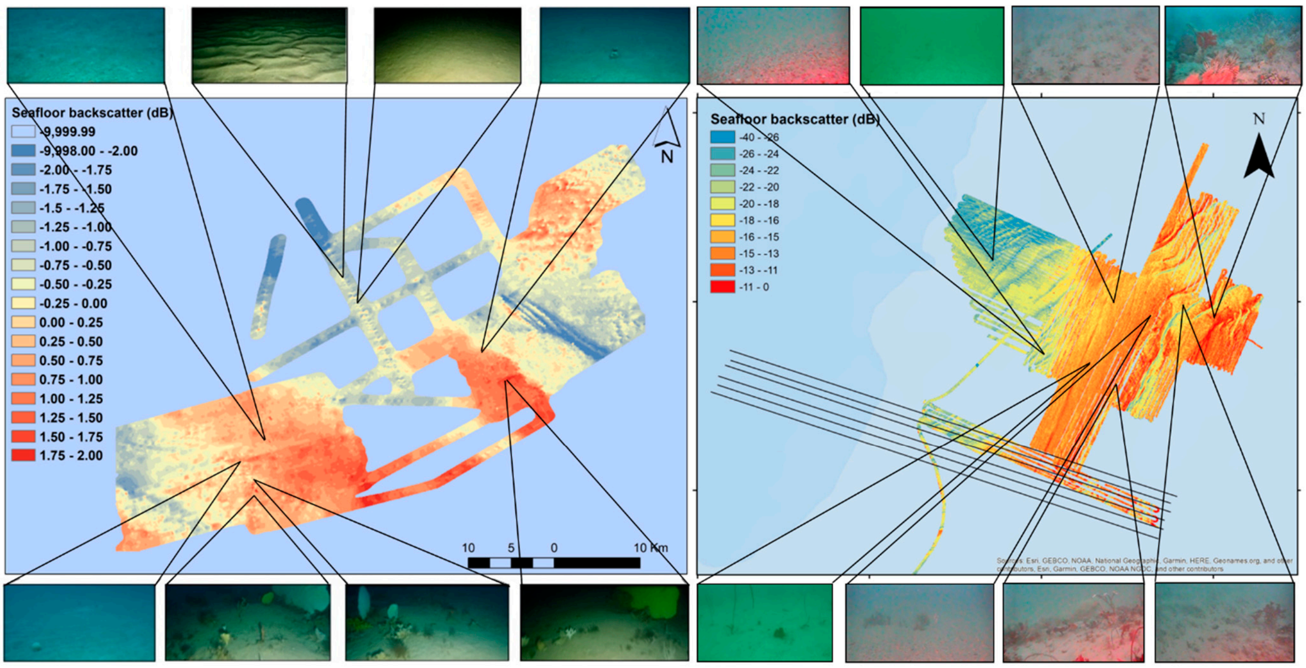


**Figure S1.** Map of sonar backscatter from a multibeam survey of the southern-deep site (left images) and the northern-shallow site (right images). Still images captured from towed video at points indicated on the map show examples of seabed corresponding to different levels of backscatter and benthic organisms (mostly sponges and gorgonians) within zones.

During the mapping survey two 15 km-long sail lines were conducted, operating a single airgun using the passive acoustic sensors to record the acoustic energy at different ranges from the airgun to confirm propagation losses at each site. A 150 cubic inch (cui) Sercel G Gun II airgun was deployed ≈ 40 m astern of the research vessel *RV Solander* and towed along these lines, at ≈ 4.5 kn at 5 m depth, with one discharge every 60 s, over a period of approximately 1.8 hours, resulting in ≈ 139 m between each of 108 discharges. Single airgun signals were recorded at ranges from tens of m to tens of km. Propagation loss within the experimental area was consistent with predictions of initial propagation models, with trends similar to, though greater than spherical spreading (i.e. $20\log_{10}(range)$, Figure S2). Propagation losses were found to be much greater at the northern inshore site, than the southern offshore site which was due to the exposed limestone reefs.

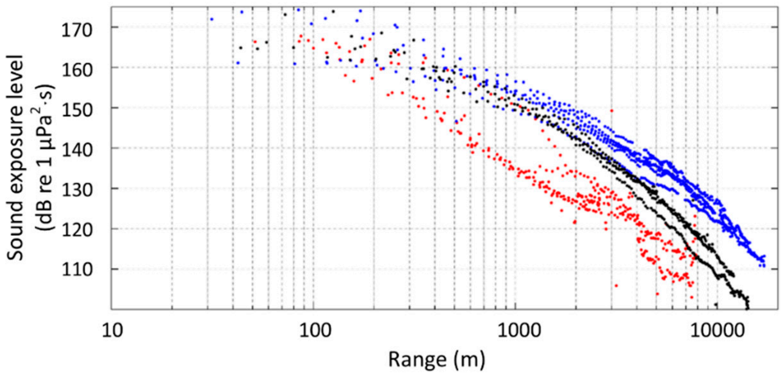


**Figure S2.** Sound exposure levels with range of a 150 cui airgun towed and discharged every 60 s along one transect at the northern site (red dots) and two transects conducted at the southern site (blue – offshore side and black dots – inshore side).

*Seismic Source*

Airgun configuration and volumes for the 2600 cui array used during the exposure period can be found in Figure S3 and Table S1, whereas operational details of the seismic survey can be found in Table S2.

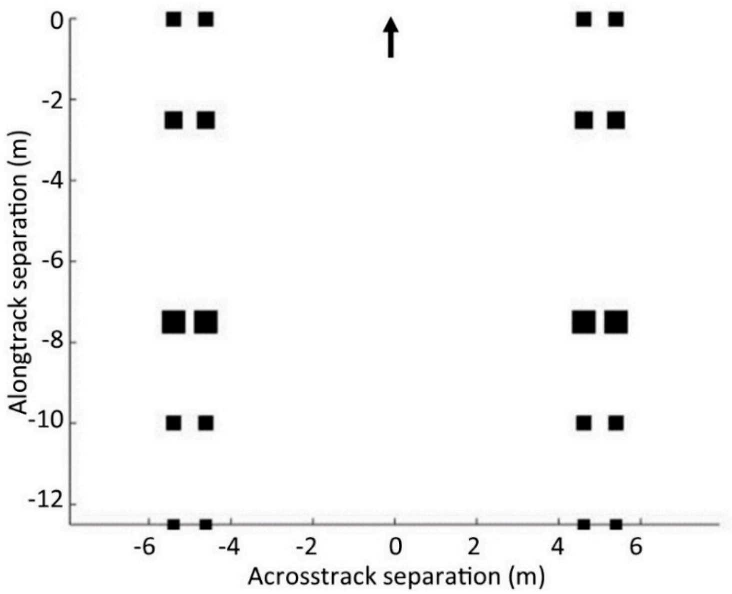


**Figure S3.** Airgun (black squares) positions and sizes for the 2600 cui arrays towed by *BGP Explorer* where size of marker has been scaled to reflect the relative volume of the airgun and arrow denotes direction of travel.

**Table S1.** Configuration of each 2600 cui array, where X is the across-track axis (negative to port and positive to starboard direction, referenced to the centreline of the vessel) and Y is the along-track axis (positive to forward, referenced to the forward guns).

| Port string | | | | Starboard string | | | |
|---|---|---|---|---|---|---|---|
| Airgun # | x (m) | y (m) | Volume (cui) | Airgun # | x (m) | y (m) | Volume (cui) |
| 4 | -5.4 | 0 | 100 | 1 | 5.4 | 0 | 100 |
| 3 | -4.6 | 0 | 100 | 2 | 4.6 | 0 | 100 |
| 8 | -5.4 | -2.5 | 150 | 5 | 5.4 | -2.5 | 150 |
| 7 | -4.6 | -2.5 | 150 | 6 | 4.6 | -2.5 | 150 |
| 12 | -5.4 | -7.5 | 250 | 9 | 5.4 | -7.5 | 250 |
| 11 | -4.6 | -7.5 | 250 | 10 | 4.6 | -7.5 | 250 |
| 16 | -5.4 | -10 | 90 | 13 | 5.4 | -10 | 90 |
| 15 | -4.6 | -10 | 90 | 14 | 4.6 | -10 | 90 |
| 20 | -5.4 | -12.5 | 60 | 17 | 5.4 | -12.5 | 60 |
| 19 | -4.6 | -12.5 | 60 | 18 | 4.6 | -12.5 | 60 |

**Table S2.** Characteristics of seismic vessel operations at each experimental site.

| **Characteristic** | **Southern site** | **Northern site** |
|---|---|---|
| Vessel speed | ≈4.5 kn (8.5 kmph) | ≈4.5 kn (8.5 kmph) |
| Sequential line separation | 500 m | 500 m |
| Sail line length (km) | 15 (minimum), | 20 (ideal) |
| Time per line (hrs) | 1.8 hrs | 2.4 hrs |
| Number lines (active) | 8 | 6 |
| Number lines (inactive) | 8 | 0 |
| Sequential line separation (time) | 12-13 hours | 24 hrs (two lines) 12 hrs (4 four lines) |
| Discharges per line | 1200 | 1600 |
| Discharge spacing (time) | 5.5-6 s (speed dependent) | 5.5-6 s (speed dependent) |
| Discharge spacing (distance) | 12.5 m | 12.5 m |

The modelled source of the far-field waveform, power spectral density and array beam directivity pattern (plan at 60 Hz, along-track at 50 Hz and across-track at 50 Hz) are shown in Figures S4 and S5, whereas specifications of the *BGP Explorer* can be found in Table 3.

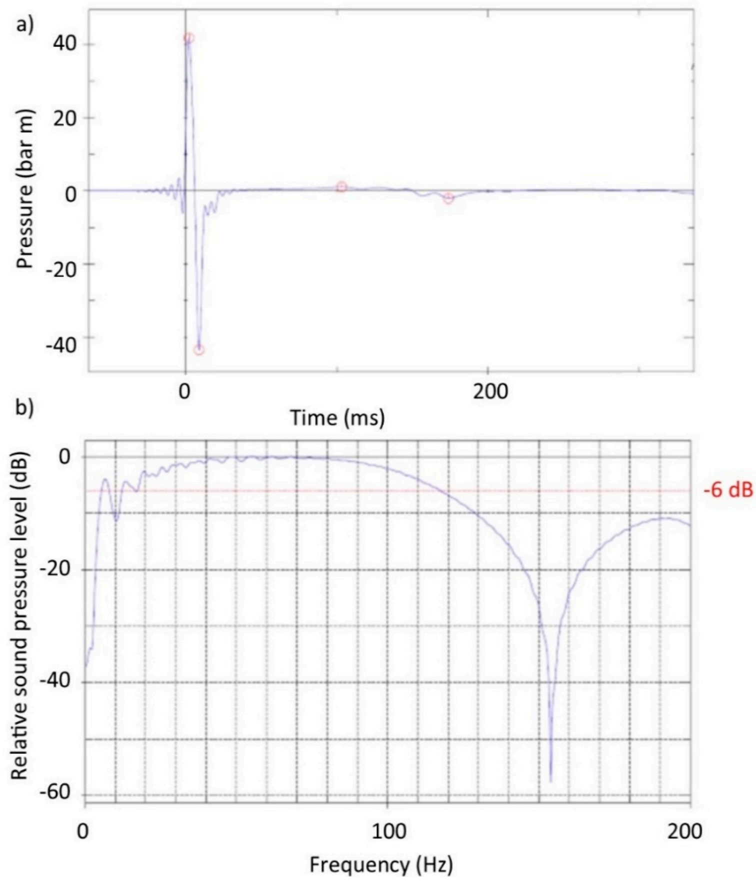


**Figure S4.** Modelled (PGS Nucleus model) source signal waveform (a) and relative power spectral density (b) for the far-field signature of the 2600 cui airgun array signal (5 m source depth, 41.8 bar m primary pressure). Red line in (b) marks the -6 dB limit. Images supplied by Exploiter PTE. LTD.

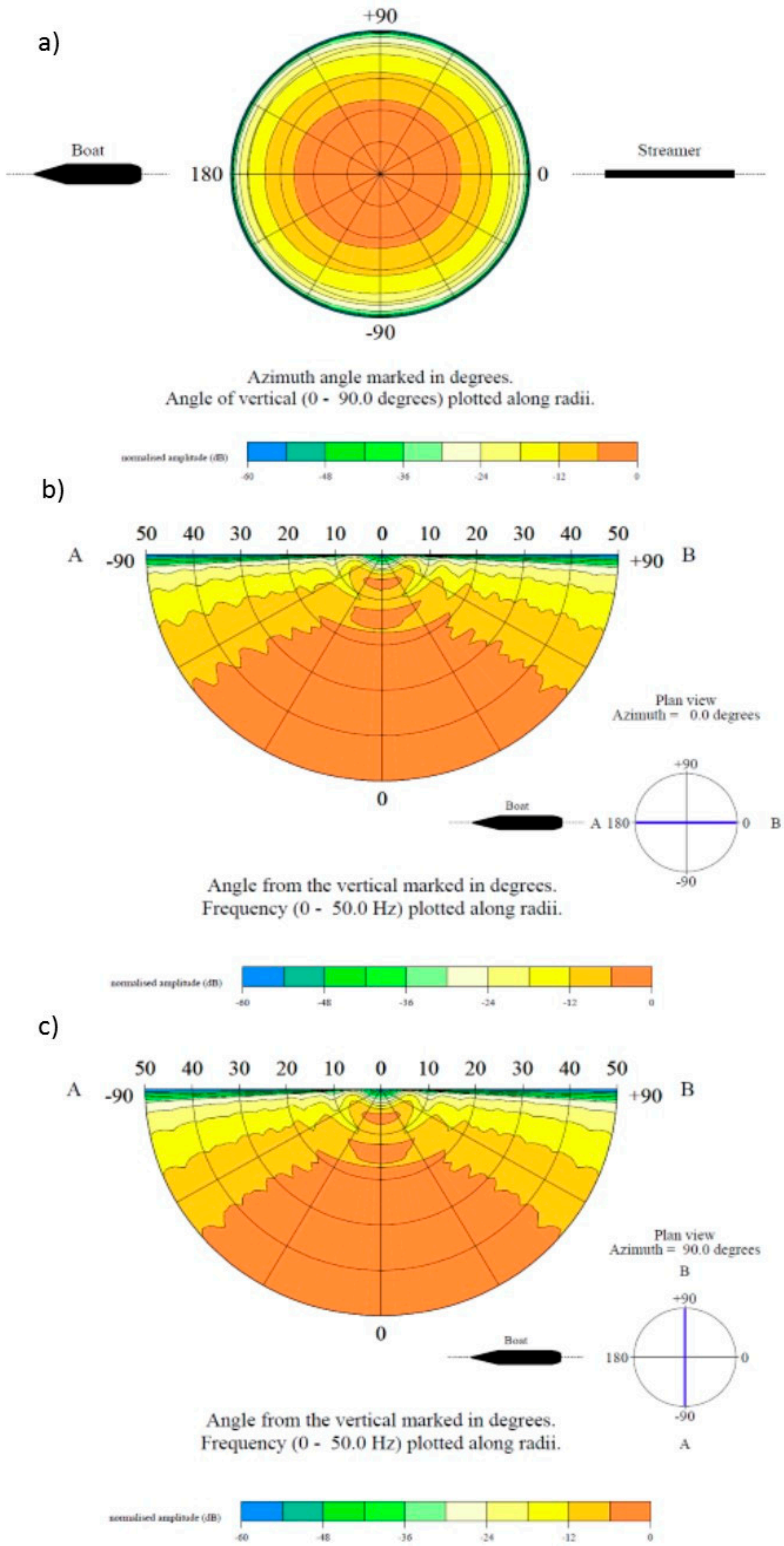


**Figure S5.** Modelled (PGS Nucleus) airgun array signal directivity patterns for (a) horizontal plane directivity at 60 Hz, (b) vertical plane along-track directivity at 50 Hz, and (c) vertical plane across-track directivity at 50 Hz. Images supplied by Exploiter PTE. LTD.

**Table S3.** Details of the source vessel, *MV BGP Explorer.*

| | |
|---|---|
| Flag: | Panama |
| Class: | ABS / CCS |
| Year of Built: | 2010 |
| Length: | 64 m |
| Breadth: | 16 m |
| Draft (min / max): | 4.35 m / 4.75m |
| Gross Tonnage: | 2800 |
| Speed: | 12 knots |
| Fuel Capacity: | 700.5 $m^3$ |
| Main engine: | Niigata 6MG25HX, 2 x 1800 BHP |
| Bow Thruster: | 5.0 T fixed pitch type |
| Auxiliary Engines: | Volvo D12-AUX 2 x 250 BHP |
| Generators: | 2 x 245 kw, 2 x 500 kw |
| Propeller Type: | 2 sets, fixed pitch propeller |

*Acoustics sensors and measurements*

An example calibration curve for three USRs can be found in Figure S6.

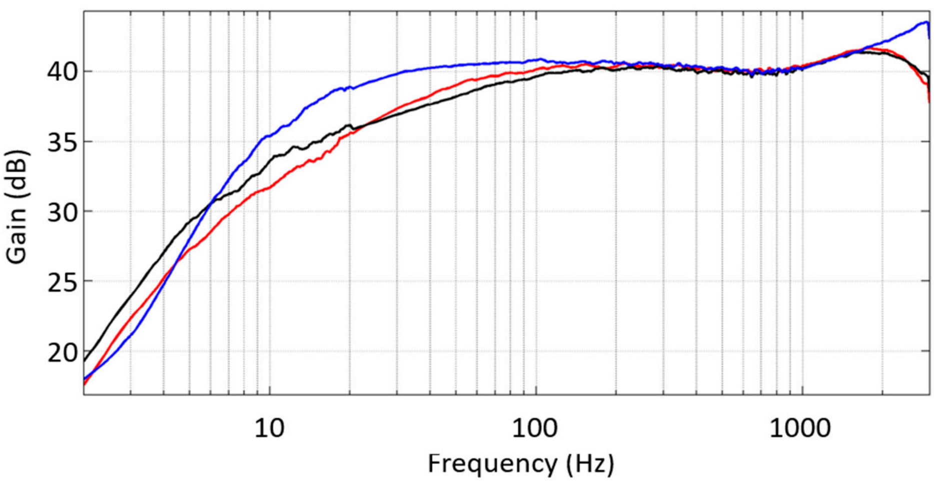


**Figure S6.** Example of system gains with frequency response for USRs from the white noise injection calibration.

Ambient noise levels for the different acoustics metrics can be found in Figure S7, whereas sound exposure levels from an example seismic sail line conducted at the northern and southern sites can be found in Figures S8 and S9, respectively. Periods where ambient noise levels were measured were split into five second windows (4851 samples) and analysed to provide a measure for each acoustic metric. Ground acceleration values for background noise could not be calculated as the noise floor of the instrument was above ambient levels. The levels at locations where the airgun array signal had attenuated to near or below ambient levels of noise or during times when the seismic vessel was not present, provided a baseline with which the airgun signals detected elsewhere could be compared.

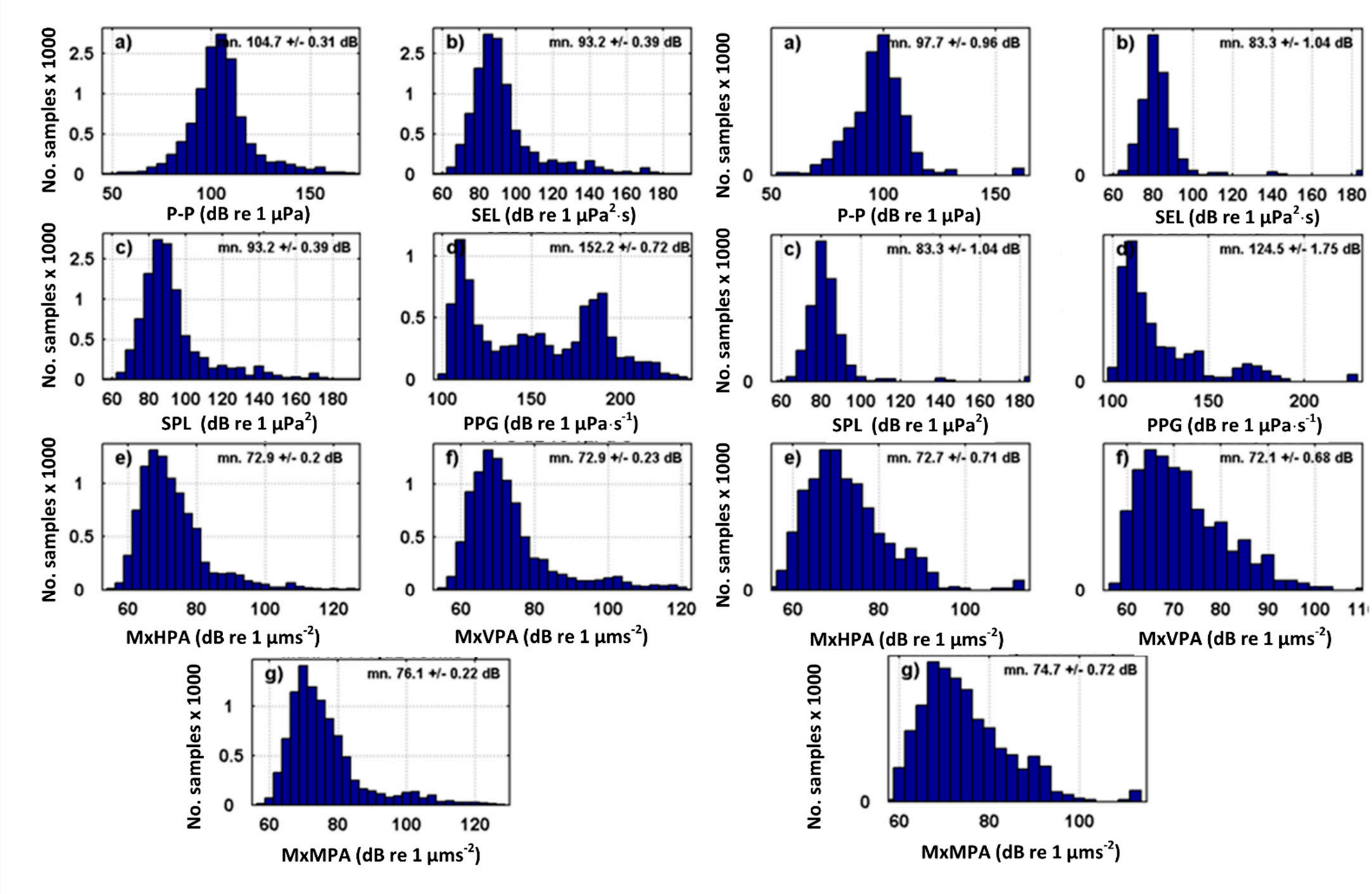


**Figure S7.** Distribution of ambient noise levels for peak-to-peak pressure level (a), sound exposure level (b), mean-square sound pressure level (c), PPG (d), maximum horizontal particle acceleration (e), maximum vertical particle acceleration (f) and maximum magnitude of particle acceleration (g) at the northern (left columns) and southern (right columns) sites.

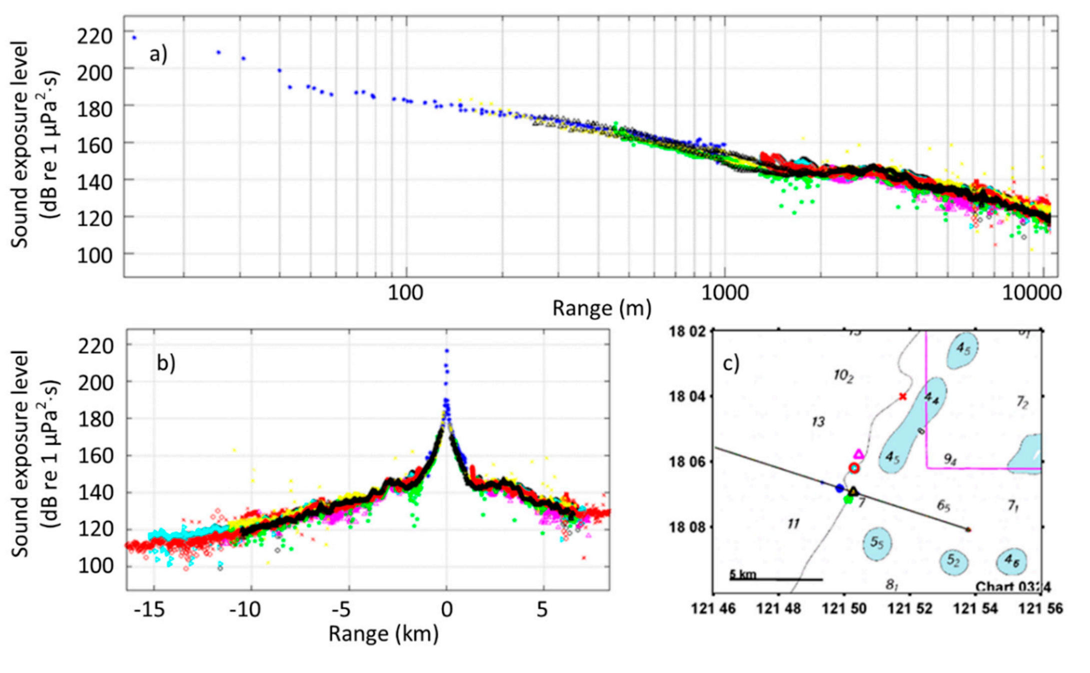


**Figure S8.** Sound exposure levels with range for a seismic sail line operated at the northern site on 18th September 2018 ((a) and (b)) by USRs positioned at various distances from the sail line. Coloured dots relate to the USR datasets from the recording positions shown in c) using the respective colours from (a) and (b).

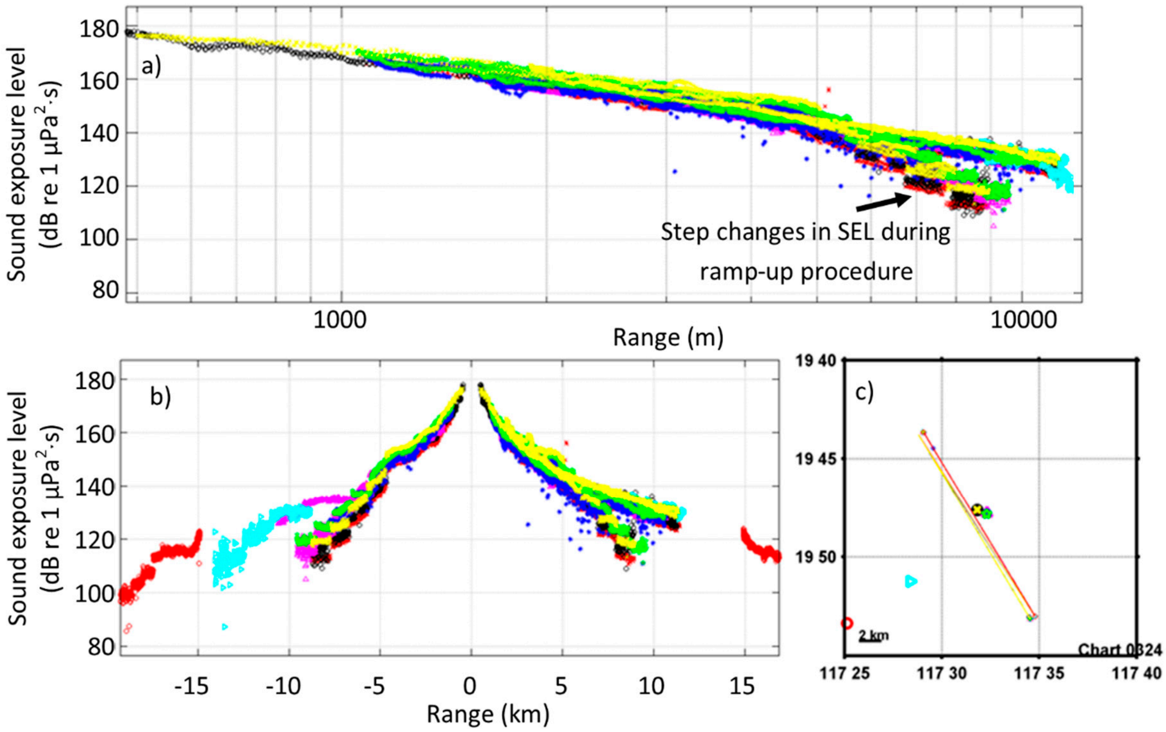


**Figure S9.** Sound exposure levels with range for a seismic sail line operated at the southern site on 23rd September 2018 ((a) and (b)) by USRs positioned at various distances from the sail line. Coloured dots relate to the USR datasets from the recording positions shown in (c) using the respective colours from (a) and( b). Periods where an increasing number of guns were operated prior to the start of the seismic sail line (i.e. the 'ramp-up') are highlighted.

*Ancilliary data*

- Sound propagation models require information on geophysical properties within the water column. Vertical oceanographic profiles were made using the RV Solander, Sea-Bird SBE 9 profiler mounted on a rosette. This instrument is calibrated and maintained by AIMS. Parameters measured included: temperature; pressure; conductivity; fluorescence; sediment load using Beam Transmission with a WET Labs C-Star; density; and light transmission (PAR).
- Unless stated otherwise all times are UTC.
- All analysis uses purpose-built software run in MATLAB (The MathWorks Inc.).
- Bathymetry was calculated using the 0.0025° Geoscience Australia grid [42].
- Spatial analysis uses the MATLAB mapping toolbox using latitude and longitude on great circle paths with WGS 84 chart datum.
- All charts displayed are from the Australian Hydrographic Service under Seafarer GeoTIFF Curtin University license No 2618SG.
- Tidal predictions used WXTide 4.7 for Primary Ports with the tidal time adjusted for the location.